University of Alberta

Influence Of Alcohol Fuel Additives On Strain Measurements In Glass Fiber-Reinforced Micro-Specimens.

By

Allen Yong Lian Goh

A thesis submitted to the Faculty of Graduate Studies and Research in partial fulfillment of the requirements for the degree of Master of Science

Department of Mechanical Engineering

Edmonton, Alberta

Fall 2000

National Library of Canada
Acquisitions and Bibliographic Services
395 Wellington Street
Ottawa ON K1A 0N4
Canada

Bibliothèque nationale du Canada
Acquisitions et services bibliographiques
395, rue Wellington
Ottawa ON K1A 0N4
Canada

Your file Votre référence

Our file Notre référence

The author has granted a non-exclusive licence allowing the National Library of Canada to reproduce, loan, distribute or sell copies of this thesis in microform, paper or electronic formats.

The author retains ownership of the copyright in this thesis. Neither the thesis nor substantial extracts from it may be printed or otherwise reproduced without the author's permission.

L'auteur a accordé une licence non exclusive permettant à la Bibliothèque nationale du Canada de reproduire, prêter, distribuer ou vendre des copies de cette thèse sous la forme de microfiche/film, de reproduction sur papier ou sur format électronique.

L'auteur conserve la propriété du droit d'auteur qui protège cette thèse. Ni la thèse ni des extraits substantiels de celle-ci ne doivent être imprimés ou autrement reproduits sans son autorisation.

0-612-59807-1

Canada

University of Alberta

Library Release Form

Name of Author: Allen Yong Lian Goh

Title of Thesis: Influence of alcohol fuel additives on strain measurements in glass fiber-reinforced micro-specimens.

Degree: Master of Science

Year this Degree Granted: 2000

Permission is hereby granted to the University of Alberta Library to reproduce single copies of this thesis and to lend or sell such copies for private, scholarly or scientific research purposes only.

The author reserves all other publication and other rights in association with the copyright in the thesis, and except as herein before provided, neither the thesis nor any substantial portion thereof may be printed or otherwise reproduced in any material form whatever without the author's prior written permission.

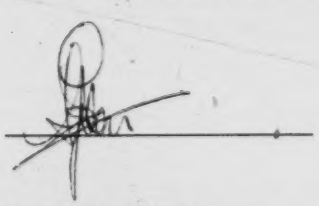

203, 10732 86 Avenue
Edmonton, Alberta
T6E 2M9

Date: 6th October 2000

University of Alberta

Faculty of Graduate Studies and Research

The undersigned certify that they have read, and recommend to the Faculty of Graduate Studies and Research for acceptance, a thesis entitled **Influence of alcohol fuel additives on strain measurements in glass fiber-reinforced micro-specimens**. submitted by **Allen Yong Lian Goh,** in partial fulfillment of the requirements for the degree of Master of Science.

A. Bhattacharyya

Dr. A. Bhattacharyya
Mechanical Engineering

Dr. T. Forest
Mechanical Engineering

Dr. B. Jar
Mechanical Engineering

Dr. P. Choi
Chemical & Materials Engineering

Date: 2nd October 2000

ABSTRACT

This dissertation addresses the effects of alcohol additives in hydrocarbon fuels on the mechanical properties of fiber reinforced plastics (FRP). The study focused on testing thin (~254 μm) composite tensile specimens to accelerate the time required to achieve saturation. A non-contact optical method was developed to measure the change in distance between two aluminium strips sputter-deposited along the gauge width of each specimen. Extensional strain is inferred from this measurement.

An exposure time of 3 and 7 days of the specimens to the fuel mixture, as compared to virgin-state specimens, showed considerably lower flow stress at 1.5% strain. Flow stress recovers significantly when the exposed specimens are dried for 3 and 7 days respectively. These results point to two possibilities: 1. Design of FRP structures exposed to alcohol-based fuels has to account for noticeable mechanical property changes during the service period, and 2. Property changes may be partially reversed by "drying" the structures over an appropriate period of time.

ACKNOWLEDGEMENTS

I would like to express my sincere appreciation to my supervisors, Dr. Abhijit Bhattacharyya, and Dr. Tom Forest, for their guidance and mentorship. I would also like to thank:

Mr. Gary Steadman of RP Composites in Sherwood Park for his advice, help and support in obtaining the necessary resin mix.

The Natural Sciences and Engineering Research Council for partial financial support.

The machinists: Albert Yuen, Don Fuhr, Tony Van Straten and David Pape for their ideas and superior craftsmanship in designing and making my resin mold.

The technical staff: Ian Buttar, Bernie Faulkner, Tuula Hilvo and Terry Nord. I would especially like to thank Bernie for his creativity and patience during the experimental part of the research.

Dr. Mark McDermott and James Kariuki from the Department of Chemistry for their assistance in determining the surface structure of my samples.

Mary Seto from the Department of Electrical and Computer Engineering for her guidance in sputter deposition.

The University of Alberta Microfab staff for their support and use of their equipment.

Dr. David Budney for listening to my ideas, providing me with his opinions and ideas.

My colleagues, Julian Amalraj, Emmanuel Appiah, Vesselin Stoilov, and Sandra Esteves for all the small but invaluable tips and ideas.

Nicholas Sun, my summer student, for his help in preparing the test samples.

Yen Linh, my inspiration and driving force. This would not be possible without her encouragement and patience.

Last but not least my parents, Hon Chuan and Teresa, and my brother Kelvin, for their constant support and belief in me.

TABLE OF CONTENTS

CHAPTER 1
INTRODUCTION 1

CHAPTER 2
COMPOSITE TENSILE MICRO-SPECIMEN PREPARATION TECHNIQUES 12
2.1 Preparation of thin composite sheets 12
2.2 Sputter Deposition of Thin Aluminium Strips 14
2.3 Cutting of Tensile Micro-Specimens 15

CHAPTER 3
ANALYSIS OF THE SURFACE OF THE SPUTTERED PLASTIC SHEETS 16
3.1 Equipment and Procedure 16
3.2 Observations and Discussion of Results 17

CHAPTER 4
THE TEST PROCEDURE AND STRAIN MEASUREMENT TECHNIQUES 20
4.1 Test procedure 20
4.2 Tensile testing of the micro-specimens 22
4.3 Determination of extensional strains 23

CHAPTER 5
TEST RESULTS AND DISCUSSIONS 27

CHAPTER 6
CONCLUSIONS AND FUTURE WORK 32

REFERENCES 34

APPENDIX
PREPARATION OF MASK FOR SPUTTERING 37

LIST OF FIGURES

Figure 1: (a) Schematic of the tensile micro-specimen, with dimensions conforming to ASTM D638M-93, (b) An enlarged view of the gauge section. 38

Figure 2: Schematic of the steel mold used to make fiber-reinforced composite sheets. 39

Figure 3: (a) Schematic of a composite sheet with two aluminium strips, (b) An exploded view of the assembly used to produce the sputtered sheets. 40

Figure 4: Schematic of the template used to cut the tensile micro-specimens. 41

Figure 5: Scanning Force Microscopy (SFM) images: 42

A. Bare surface of a composite sheet before exposure to alcohol-based fuels,

B. Aluminium covered surface of a composite sheet before exposure to alcohol-based fuels,

C. Bare surface of a composite sheet after 7 day exposure to a volumetric mixture of 50%-50% methanol-ASTM Fuel C,

D. Aluminium covered surface of a composite sheet after 7 day exposure to a volumetric mixture of 50%-50% methanol-ASTM Fuel C.

Figure 6: Schematic of the configuration to test tensile micro-specimens. 43

Figure 7: A scanned image of the aluminium strip-covered surface of a tensile micro-specimen (light area: aluminium, dark area: resin). 44

Figure 8: Stress-strain curves obtained for the same micro-specimen based on strain gauge measurements, the current approach and crosshead displacements. 45

Figure 9: Stress-strain curves obtained by the current approach for 10 different micro-specimens. 46

Figure 10: Individual stress-strain curves of virgin micro-specimens. Each micro-specimen was tested to failure. 47

Figure 11: The representative stress-strain curve of the virgin FRP. 48

Figure 12: Individual stress-strain curves of micro-specimens after 3-day exposure to fuel mixture. Each micro-specimen was tested to failure. 49

Figure 13: Individual stress-strain curves of micro-specimens after 7-day exposure to fuel mixture. Each micro-specimen was tested to failure. 50

Figure 14: Individual stress-strain curves of micro-specimens after 3-day exposure to fuel mixture and then drying for 3 days. Each micro-specimen was tested to failure. 51

Figure 15: Individual stress-strain curves of micro-specimens after 7-day exposure to fuel mixture and then drying for 7 days. Each micro-specimen was tested to failure. 52

Figure 16: The representative stress-strain curve of the exposed FRPs. 53

Figure 17: The representative stress-strain curve of the exposed & dried FRPs. 54

Figure 18: Dependence of the FRP flow stress (at 1.5% strain) on fuel exposure time. 55

CHAPTER 1

INTRODUCTION

Underground fuel storage tanks have been in service for over 70 years. They are widely used as they offer a safeguard against fire hazards and are space efficient. In the early years these tanks were made of steel, with or without what was then assumed to be adequate protective coating. There were many reported environmental cases that showed a connection between leakage to internal and external corrosion of these steel tanks. Skabo et al.[1], Garrity[2], and Pim[3], have conducted studies which indicated that these steel tanks began leaking after 15 years of service. An extensive U.S. Environmental Protection Agency report documented that up to 10% of underground storage tanks leaked due to internal corrosion[4]. The concern at hand was whether the gasoline fuel was responsible for the leakage. Normally, fuels such as gasoline, diesel fuels, and heating fuels are not corrosive towards steel. Bodger[5] has documented that fuel is not the cause of the corrosive attacks but rather water or aqueous salt solution deposited at the bottom of the tanks during fuel transportation. He has further researched that internal corrosion has indeed been a significant cause of leakage in underground storage tanks. Possible detrimental environment effects to the environment resulted in environmental regulations for underground fuel storage tanks[6].

In the early 1960's, fiber-reinforced plastic (FRP) tanks that eliminated corrosion-induced leakage were introduced. FRP is not susceptible to the corrosive attacks of steel, making it a better fabrication material or as a protective coating for steel tanks. Further, Skabo et al.[1], Fitzgerald[7] and Kamody et al.[8] reported that gasoline has little or no effect on the FRP tanks. In addition, Bodger's[5] study further emphasized that coating the steel tanks with FRP, particularly the bottom one-third where the aqueous salt solution is deposited, is crucial for the best protection against leakage. Cathodic protection has also been widely used to prevent internal and external corrosion of underground storage tanks. However, Stapleton[9] has reported that in Sweden, regulatory agencies believe that FRP coatings are more reliable than cathodic protection against internal protection.

Alcohols such as methanol and ethanol are being used as additives in fuel to improve octane values and to reduce harmful emissions of carbon monoxide and hydrocarbons. It is of interest to know how well the FRP, as a structural material, can withstand exposure to an aggressive environment posed by alcohol-based fuels. Specific issues of concern are:

a) What is the extent of the alcohol-based fuel diffusion into the FRP and is there any strength degradation of the FRP due to such diffusion? This

will yield information regarding the integrity of tanks when FRPs are used as the structural material.

b) If the strength degradation does occur, is it possible to reverse the effect by stopping the exposure to the fuel and allowing the FRP to "dry"?

c) Is there any leakage of fuel into the environment?

Some of these issues have been addressed by Kamody et al.[8]. In their work, Kamody et al.[8] presented useful information about the flexural strength and flexural modulus of several resin types of FRPs exposed to several alcohol-based fuels under different exposure conditions. The numerical data is presented in the form of percentage changes of the properties of the exposed FRPs with respect to the properties of the unexposed FRPs. Their tests were carried out on ASTM C-581 coupons (specific nominal dimensions of the coupons were not given in the paper). Additionally, the ambient temperature at which the experiments were conducted was 100 ^{o}F (or 37.78 ^{o}C) to accelerate the tests. A systematic research program to address the issues raised in questions (i)-(iii) above can be quite expensive and time-consuming primarily because diffusion is a slow process. This is especially true since tank wall thicknesses are typically 7 to 12 mm and the total time required in gathering reliable data may run into years.

In order to establish a connection between changes in mechanical properties of fiber-reinforced composites with the concentration of alcohol-based fuel that may have diffused into the composites, extensive and time-consuming experiments need to be carried out. A typical experiment may involve exposing a composite tensile test specimen to a certain alcohol-fuel mixture for a given period of time, and then testing the specimen in uniaxial tension to determine the uniaxial stress-strain curve. The exposure time of the alcohol-based fuel will determine the extent of fuel diffusion, and hence its concentration in the specimen. If it were possible to determine the fuel concentration within the specimen, then one could attempt to correlate the change (if any) in the stress-strain response with respect to that of the virgin composite specimen with fuel concentration.

An added complexity is that for thick specimens, there will be a concentration gradient of fuel along the specimen thickness if exposure times are relatively short. Determination of this gradient, and the subsequent correlation to changes in stress-strain response are even more difficult issues to deal with. Thus, it is desirable to make the test specimen as thin as possible, so that the assumption of a uniform fuel concentration along the specimen thickness may be made. Moreover, with diffusion being essentially a slow process (especially under ambient conditions), thin specimens are especially desirable for testing. Based on

these considerations, we have chosen to focus on tensile testing of composite micro-specimens. We use the prefix "micro" as the specimens considered are as thin as 254 μm. Schematic of the micro-specimen is shown in Figure 1, where the displayed dimensions were decided based on a specimen thickness of 254 μm, and according to the guidelines prescribed by ASTM D638M-93[10]. To get a better idea of how the amount of alcohol diffusing into the specimen varies with time, consider the transient one-dimensional diffusion into a plane slab of material. The non-dimensionalized time in the one-dimensional diffusion equation (Crank[11]) is $\frac{Dt}{d^2}$ where D is the diffusion coefficient of alcohol in plastic, d is the slab thickness, and t is time. Thus, time required to reach saturation of alcohol in plastics will vary as slab thickness squared. If we were to use normal tank wall thicknesses of 7 – 12 mm as compared to our test thickness of 254 μm, it would take us 760 – 2200 times longer to achieve the same state of saturation.

In related studies, Chin et al.[12] conducted experiments to determine the mechanical stresses of thin polyester resins after exposure to high (13.5) pH solution. This basic solution is composed of 1.8% by mass of KOH, 0.68% by mass of NaOH, and 0.5% by mass of $Ca(OH)_2$ in distilled water. They used thin specimens of 230 – 260 μm thicknesses to accelerate the test time. Their test samples were soaked for up to 350 hours at 30 and 60 °C, respectively. Prior to

tensile testing, the samples were dried under vacuum for 7 days. Their findings indicated that for samples tested at 30 °C, the amount of solution taken up by the samples leveled off after 20 hours at about 0.5% (by mass). At 60 °C, it only took about 5 hours for the test samples to level off at 0.5% solution uptake. However, there is a significant drop in solution uptake after 100 hours where it dropped almost linearly from 0.5% to 0.24% after 340 hours. This shows that there are two key factors. The first is the possibility of degradative hydrolysis which is followed by further degradation caused by cations in the basic solution depolymerizing the matrix. This basic solution dissolves a larger amount of alkali-soluble silicate glass fibers, thus allowing further penetration of the basic solution into the composite. The second factor is temperature as shown by the significant differences in water uptake corresponding to the degradation of the polymer. However, from tensile tests carried out, there were no significant changes in tensile strength as the results of the samples in basic solution is within one standard deviation of the results of the control. Because of this, the differences are not statistically significant.

Prian et al. [13] confirmed that raising the temperature is the key to accelerating the chemical degradation of the FRP. In their study, they observed that an immersion temperature of 80 °C appears to be an effective method of accelerating the degradation of FRPs without changing the corrosion mechanism.

Their results were based on experiments using E-glass/vinylester plate material in shape of rods (dimensions of 20x10x7 mm, tendon is 20 mm long and 6.2 mm in diameter) immersed in de-ionized water and in 3% ammonia. The tests were carried out at 23 °C and 80 °C respectively. They also found that the higher the pH level, the larger the degradation of the FRP. This is again caused by the depolymerization of the matrix. This is confirmed by observing the weight change of the specimens during immersion. The samples were immersed in 0.3%, 3% and 30% ammonia for 112 and 224 days respectively. The results for 0.3% ammonia showed a decrease of 0.03% in weight after 112 days but this increased to 0.04% after 224 days. As for the results for 3% and 30% ammonia, there was an increase of 0.05% and 0.45% in weight respectively after 112 days. This increased even more to 0.12% and 0.79% respectively after 224 days. These results indicate that the higher ammonia concentration solutions tend to dissolve a larger amount of glass fibers leading to further penetration of the aqueous solution into the material. Hence absorption increases leading to a net gain in weight. In comparison, Prian et al. [13] concluded that increasing the temperature was more effective than increasing the pH level in accelerating the degradation process.

In a later study, Prian et al. [14] stated that the prediction of absorption rates could not be assumed to be linear with time. They have concluded that for short term testing, the degradative ability is linear and increasing the temperature

is a valid technique to accelerating corrosion rates in tests on FRPs. However, there is a dramatic increase in degradation rates after an induction period. Their results showed that for specimens exposed at 80 °C in de-ionized water, there was a significant rate of increase in the degradation of the glass fibers after 90-100 days. For specimens exposed at 60 °C, the increase in degradation rates was noticed after about 200 days albeit not as high as the rate for 80 °C. It is this sudden degradation rate increase that makes long-term prediction of FRPs very complicated.

Craigie et al. [15] conducted experiments at room temperature (27.8 °C) and at elevated temperatures of 37.8 °C and 48.9 °C. This was done to compare and accelerate the tests that would help determine the stability and predict the life expectancy of novalac-based vinyl ester FRPs in alcohol based fuels. There was no mention of the dimensions of the test specimens. Exposure to pure methanol (100% methanol) and to a high methanol content fuel (85% methanol, 10% gasoline and 5% tert-butyl alcohol) revealed that there was very little differences in terms of weight gained (about 8% by weight). This indicates that the effect on the FRP was the same in high alcohol content fuels as in pure methanol. At elevated temperatures, the rate of weight gained was quicker at 37.8 °C and 48.9 °C compared to that of room temperature (27.8 °C). However, the weight gained (at about 10%) eventually stabilized after 1700 hours for all three cases. This

indicates that regardless of temperature, the final weight gain remained the same. This was verified with tests on the flexural properties. The flexural strength and modulus retention stabilized after 1700 hours for three test temperature conditions. Their conclusion was that after 1700 hours, there were no further changes occurring within the composite. Furthermore, chemical analysis showed no detectable changes in the chemical structure of the composite. There was no mention as to what type of chemical analysis was performed.

With the current experimental technique, an immediate question that arises during tensile testing of micro-specimens (Figure 1) is how is extensional strain going to be measured? Whatever technique is adopted should be capable of delivering an accurate measure of the strain in such small specimens and it should also be convenient enough so that the measurements may be carried out quickly and easily after the sample is soaked in fuel for a certain period of time. Chin et al.[12] adopted thin specimens as in our study; however, they did not report strain in the thin polyester samples due to uncertainty in their strain measurement technique.

Conventional strain measurement techniques using strain gauges or extensometers may not be reliable as their physical size is of a similar order of magnitude as the width and thickness of the micro-specimens considered here,

and thus may influence the deformation characteristics of the composite[16]. Another disadvantage is that exposure to fuel may adversely affect the strength of the bond between the strain gauge (or extensometer) and the sample. An alternative, but very expensive, approach is to use an electro-optical extensometer that uses a non-contact optical method to track the motion of a target (or a mark) on the micro-specimen. Another approach was reported by Goertzen[17] who used a video camera-based, non-contact, optical system to track the motion of 75 μm graphite particles glued to the surface of a tensile soft biological tissue specimen. While this approach could have been considered here, one will have to make sure that the adhesive is insensitive when exposed to alcohol-based fuels.

In this dissertation, we report an experimental technique to measure extensional strains in composite micro-specimens that is accurate, inexpensive and is not dependent on whether the micro-specimens have or have not been exposed to alcohol-based fuels. The approach involves sputter-depositing thin aluminum strips on the micro-specimens (see Figure 1(b)), and using a non-contact optical method to track the changes in the strip dimensions with tensile loading. The topography of the aluminium strips is qualitatively studied by examining the specimen surface using scanning force microscopy (SFM). The objective is to determine whether the presence of the aluminum strips will influence the deformation characteristics of the composite. As well, SFM is used

to ascertain whether the condition of the aluminium strips is affected by exposure to alcohol-based fuels.

The results of the uniaxial tensile response (stress-strain curve) of glass-fiber reinforced resins after exposure to methanol-based fuels in an ambient temperature environment are then discussed. These results are to be viewed as preliminary and part of a wider study where the influence of other parameters – specimen thickness, type of alcohol, alcohol/fuel ratio, pressure and temperature – should be studied.

This thesis has 6 sections: Section 2 discusses the composite tensile micro-specimen preparation techniques, Section 3 gives an analysis of the specimen surface, Section 4 gives details of the procedure for tensile testing and the methodology to determine extensional strains, Section 5 gives the test results and the accompanying analysis, and Section 6 states the conclusions and also includes a discussion on future work.

CHAPTER 2

COMPOSITE TENSILE MICRO-SPECIMEN PREPARATION TECHNIQUES

The technique required to prepare the composite tensile micro-specimen, as shown in Figure 1 consists of 3 steps: (i) preparation of thin composite sheets, (ii) sputter deposition of aluminium strips on the composite sheets, and (iii) cutting of tensile specimens from the composite sheets. These steps are described below in detail.

2.1 Preparation of thin composite sheets

The resin used in this research was ATLAC 490, a polyester resin supplied by ZCL Composites Inc., Edmonton, Canada. As well, the guidelines for the preparation of thin composite sheets were given by ZCL. Atlas Europol developed the resin with improved resistance to diffusion of alcohol-based fuels[8]. Non-woven glass fiber (randomly oriented) mats with a nominal thickness of 254 μm were used. In order to make the composite sheets, a steel mold was fabricated according to the schematic in Figure 2. The upper surface of the bottom part of the mold is machine polished to produce a smooth layer on which the glass fiber sheet-resin combination will be placed. A channel is cut along the outer edge of the polished surface. The mold has a top part that is identical to the bottom part

with the difference being the top part has run-off channels (see Figure 2). The channels filter out the excess resin during the molding process to produce a uniform thin sheet of the composite.

The first step in the molding process involves polishing the inner surfaces (see Figure 2) of the bottom and top parts of the mold with a wax (commercial name is Honeywax, made by Specialty Products Company Ltd.). This wax acts as a release agent when the composite sheet needs to be peeled off after the molding process is complete. Four layers of wax are applied to enable quick and easy release of the sheet. After polishing, the resin mix was prepared with the addition of 2.5% (by weight) of catalyst (Superox 46-747 MEKP Peroxide) to accelerate the curing of the resin. Approximately 200 stirring cycles were used to ensure the catalyst was completely and evenly blended in with the resin. The catalyst-resin mix was then poured on to the upper surface (depth: 254 μm) of the bottom part of the mold to obtain a thin layer. Despite taking deliberate care, some air bubbles are formed during the preparation of the catalyst-resin mix. That is why the pouring of the catalyst-resin mix into the mold has to be done slowly so as to minimize the amount of air bubbles that are transferred into the mold. In order to get a uniform thin layer of resin, it was allowed to evenly spread out by the simple method of slanting the mold in different directions successively. This process had to be completed in less than 20 minutes, as that was the setting time of the resin.

Finally, a non-woven glass fiber mat (cut to the nominal dimensions, 110 mm x 190 mm, of the upper surface of the bottom part of the mold) is laid over the resin layer, and the top part of the mold is then bolted down onto the bottom part. The mold is then put into a preheated oven for 1 hour at 60 °C for curing, after which it is removed and allowed to remain at room temperature (20 °C) for 18 hours. The thin composite sheet with a nominal thickness of 254 μm may now be easily removed from the mold.

2.2 Sputter Deposition of Thin Aluminium Strips

The composite sheets, prepared as described in the previous section, are sputtered with aluminum such that two strips are deposited; see schematic of Figure 3a. The width of the strips and that of the bare specimen surface between the strips are given in Figure 1(b). The two strips were deposited to determine extensional strains. This has been described in detail in Chapter 4.3. Here we describe the process of deposition of the aluminum strips.

An exploded schematic of the assembly used for sputtering is shown in Figure 3b. The mask used for sputter deposition is made from 0.0254mm (0.001 in) thick brass shimstock manufactured by Precision Brand Ltd. The details of the mask preparation are given in the Appendix. We determined that a sputtering time of 30 minutes at a pressure of 5 X 10^{-7} torr in a Kurt J. Lesker Sputter Super

System II machine is to be used. Using an aluminium target, aluminium strips that were thick enough to be visible to the naked eye were sputtered onto the composite sheets. The surface properties of these strips are discussed in Chapter 3.

2.3 Cutting of Tensile Micro-Specimens

Recall the dimensions of a typical micro-specimen, shown in Figure 1. Based on a thickness of 254 μm, the remaining dimensions are prescribed by ASTM D638M-93 titled "Standard Test Method for Tensile Properties of Plastics (Metric)". The cutting template, seen in Figure 4, is constructed from steel strips, each having a thickness of 3 mm. As a first step, each composite sheet is cut into pieces with dimensions, 12 mm x 60 mm. Two such pieces are then placed in each slot between successive steel strips at a time. Two pins are used to align the steel strips and adjustable 2 in."C" clamps are used to lock down the steel strips. The tensile micro-specimens are then cut using a high speed Dremel hand drill.

CHAPTER 3

ANALYSIS OF THE SURFACE OF THE SPUTTERED COMPOSITE SHEETS

The aluminium strips sputtered onto the composite sheets need to be thin enough compared to the thickness of the composite sheets, so that the strips do not influence the deformation characteristics of the composite. To this end, we have used scanning force microscopy (SFM) to obtain a qualitative confirmation of the relative thinness of the aluminium strips. As well, we have used SFM to study the topography of the specimen surface, and any possible changes on the surface, especially that of the aluminium strips, after the specimen is exposed to alcohol-based fuel. The SFM studies are described in the remainder of this chapter.

3.1 Equipment and Procedure

Scanning force microscopy (SFM) was employed to examine the topography of the composite sheets using a Nanoscope III Multimode (Digital Instruments, Santa Barbara, California). Samples with nominal dimensions of 1 cm x 1 cm were cut from the composite sheets so as to fit on the microscope scanner. High-resolution images are obtained by scanning the sample in ambient air under a sharp probe-tip in contact with the sample surface. The tip is

integrated with a Si_3Ni_4 cantilever (Digital Instruments, Nanoprobe) that deflects vertically in response to the sample topography. The cantilever is very flexible, exhibiting a spring constant of 0.06 nN/nm (i.e. a vertical load of 0.06 nanoNewtons at the cantilever tip causes a vertical tip deflection of 1 nanometer). The cantilever deflection is detected by a laser beam reflected off the backside of the cantilever into a position sensitive photodiode detector. Because of the sharpness of the tip (10-13 nm radius of curvature) and the ability to detect minute cantilever deflections (0.1 nm), SFM images exhibit nanometer-scale resolution in the x, y and z directions (where the x-y plane coincides with the sample surface, and the z-axis is perpendicular to the sample surface). All images were software flattened and are shown unfiltered.

3.2 Observations and Discussions of Results

SFM imaging was performed on our test samples for two purposes. The first was to assess the effect of the aluminium strip on the topography of the composite sheet. Figs.5(a) and (b) are 10 μm x 10 μm representative images of the bare surface and the aluminium strip-covered surface of a composite sheet respectively. From Figure 5(a), it appears that the topography of the bare surface is quite rough as indicated by the relatively large z-scale of the image (150 nm). Observed features include parallel troughs running diagonally across the image. We believe these troughs are the result of the mold used to fabricate the

composite sheets. In addition, a high density of pits, with diameters ranging from 50-200 nm, is observed on the surface. We have observed pits on all the composite sheets we have investigated, in some cases with diameters as large as 3 μm. From the point of view of the mechanical response of the composite specimens, it is not known whether these pits play any significant role. This has to be ascertained, and we hope to do it in the future. Figure 5(b) is a SFM image of the top of the aluminium strip-covered surface of the composite sheet. Features observed on the aluminium are very similar to those on the bare surface of the sheet. From this and other images, we conclude that the topography obtained by scanning the top of the aluminium strip-covered surface is indistinguishable from that of the bare composite surface. This provides a qualitative confirmation of the fact that the sputter-deposited layer of aluminium is extremely thin compared to the thickness of the composite sample.

The second motivation for employing SFM was to examine the effect of exposure of the test samples to alcohol-based fuels. Figs.5(c) and (d) are images of the bare surface and the aluminium strip-covered surface of a composite sheet respectively, following immersion of the sheet in a volumetric mixture of 50% methanol-50% ASTM Fuel C[1] for 7 days. We removed the sample from the fuel, dried it under a stream of Argon and imaged immediately. Comparing Figs.5(a)

[1] ASTM Fuel C is a mixture by weight of 50% isooctane and 50% toluene.

and (b) with Figs.5(c) and (d) respectively, topographic variation induced by exposure to fuel is undetectable. The pits in Figure 5(c) are larger (150-800 nm) than those in Figure 5(a), but their diameter falls in the range of pit diameter (up to 3 μm) we have observed on the bare surface of other composite sheets not exposed to the fuel. Based on this qualitative study, we infer that the exposure to the methanol-ASTM Fuel C mixture for 7 days does not affect the SFM-mapped topography of either the bare surface or the aluminium-covered surface of the composite sheets. In particular, since the aluminium strip seems to be unaffected by exposure to the methanol-ASTM Fuel C mixture, any experimental technique developed to measure strains in unexposed micro-specimens based on dimensional changes of the aluminium strips may also be used to measure strains on exposed tensile micro-specimens.

CHAPTER 4

THE TEST PROCEDURE AND STRAIN MEASUREMENT TECHNIQUES

In this chapter, the rationale and the details of the test procedure are first described, and are then followed with the strain measurement techniques.

4.1 Test procedure

The effect of exposure time of the FRP to fuel is expected to translate into specimens with different levels of saturation, accompanied with possible changes in tensile properties. For this preliminary study, we decided to focus on two exposure times that would provide two distinct levels of saturation. Motivated in part by the availability of test facilities, we chose exposure times of 3 and 7 days. The tensile properties at these exposure times turned out to be distinctly different from each other and also from that of the virgin specimens; therefore, we focussed on a 3-day and 7-day exposure time during the rest of the study. The question as to whether a 7-day exposure time is sufficient to attain full saturation is a separate issue, and will have to be verified in future work. Further, motivated by a common industry practice of allowing the tanks to dry out after a certain number of years in service, we wanted to see what sort of recovery in the tensile properties of the FRP may result if the exposed micro-specimens are left to dry

for the same period of time as the exposure time. As well, to provide a reference against which any tensile property changes may be compared, unexposed (or virgin) specimens need to be tested.

Based on the above reasons, the following tests were carried out on tensile FRP micro-specimens under an ambient temperature of 20 ^{O}C:

i. Tests of virgin specimens,

ii. Tests of specimens immediately after exposure to a 50-50 volumetric mixture of methanol and ASTM Fuel C (referred hereafter as the "fuel mixture") for a period of 3 days.

iii. Tests of specimens exposed to the fuel mixture for 3 days, and then dried in ambient conditions for 3 days.

iv. Repetition of Steps ii and iii above for specimens with exposure time of 7 days.

We found that the micro-specimens that are supposed to be tested immediately after fuel exposure do regain their tensile property during the short period of time it took to retrieve the specimen from the fuel mixture, load it onto the test frame and begin testing. We drew this inference by comparing the obtained results with those from specimens that are wetted with the fuel mixture while being loaded onto the test frame. The latter approach is probably more

preferable (for Step ii above). Therefore, for all micro-specimens tested immediately after exposure to the fuel mixture, we allowed the fuel mixture to drip onto the specimen during its loading onto the test frame. However, when the tensile testing began, the dripping was terminated as otherwise it hindered the data collection.

4.2 Tensile testing of the micro-specimens

Schematic of the configuration to test the micro-specimens is shown in Figure 6. The tensile tests were carried out on a Instron TTK testing machine. Custom-made steel serrated grips were used to hold the micro-specimens. A non-contact optical system (a microscope mounted camera with 10 times magnification) was used to photograph the aluminium strip-covered surface of the tensile test specimen at regular intervals during the test process. The test specimens were subjected to a deformation-controlled process, at a rate of 0.508 mm/min (0.02 in/min). This rate was chosen based on convenience and on the speed setting of the Instron TTK testing machine. The next higher speed setting of 1.27 mm/min (0.05 in/min) available on the machine made it difficult to prepare the camera between the interval-controlled snapshots. At lower rates (0.254 mm/min (0.01 in/min) and below), there is a possibility that specimens may dry during the time it took for tensile testing to complete. The average time taken for each specimen from test initiation to failure was about 90 seconds when tested at

0.508mm/min. A timer was used to record the onset of testing and its progress to failure, and the camera was used to photograph the aluminium strip-covered specimen surface at intervals of 10 seconds. The load on the specimen was sampled by the load cell and recorded by a digital recorder every 0.4 seconds. In order to achieve synchronization, the camera was also connected to the digital recorder whereby it was possible to exactly match each photograph with the correct load. The photographs of the specimen surface are later used to prepare slides, which, in turn, are used to determine the extensional strains in the micro-specimens. This is addressed in the next section.

4.3 Determination of extensional strains

The following is an explanation of extensional strains and the corresponding stresses that develop during tensile testing of the micro-specimens. Let us assume that over the time span from test initiation to failure of each micro-specimen, a total of N photographs is taken. Let us denote the stress and strain corresponding to the ith photograph ($1 \leq i \leq N$) as σ_i and ε_i respectively. For all specimens, $i = 1$ corresponds to the no-load situation at test initiation, i.e. $\sigma_i = 0$. The stress is defined as

$$\sigma_i = \frac{P_i}{A}, \qquad (1)$$

where P_i is the load on the micro-specimen when the ith photograph was taken,

A is the original cross-sectional gauge area of the specimen (typically 0.635 mm^2).

The strain, ε_i, is determined from the ith photograph in the following manner. The slide corresponding to the ith photograph is projected on a screen using an overhead projector; we determined that the image on the screen was magnified 25 times that of the image in the slide (and therefore magnified 250 times the size of the actual specimen surface). An example of such an image is shown in Figure 7. The dark surface corresponds to the resin whereas the light surface corresponds to the aluminium strips. These strips have essentially been used as "markers" to help track the deformation of the bare resin surface (dark surface in Figure 7). A pair of locations, one at the top edge of the dark surface and the other at the bottom edge shown on the figure as A and B, are selected in such a way that these locations can also be identified on all the images ($1 \leq i \leq N$) corresponding to the tensile test specimen under consideration. Further, the pair is chosen in such a way that the line AB is along the tensile loading direction. In this manner, we identified a minimum of three pairs of points (and up to a maximum of 5 pairs) on each photograph of a tensile test specimen. Therefore, each pair of points on the ith photograph will be denoted as A_i^j and B_i^j ($1 \leq i \leq M$). Defining

AB_i^j as the length between the points A_i^j and B_i^j, we find the average of the lengths for the *M* pairs of points, and compare this length for the *i*th photograph to the length for the first photograph (no-load condition) to obtain the extensional strain. Mathematically, the extensional strain is defined as

$$\varepsilon_i = \frac{\sum_{j=1}^{M} AB_i^j}{\sum_{j=1}^{M} AB_1^j} - 1, \qquad (2)$$

The values, σ_i and ε_i ($1 \le i \le N$), determined from Eqs.1 and 2 give the stress-strain curve for a typical micro-specimen. We determined that the major source of error in the stress was the measurement of the cross-sectional area of each specimen whereas the major source of error in the strain was the measurement of the length of AB_i^j (see previous section). Based on an error analysis, we found that the absolute values of the errors, $\Delta\sigma$ and $\Delta\varepsilon$, in the stress and strain respectively were bracketed within the ranges, $\pm 0.1994 \le \Delta\sigma \le \pm 0.625$ MPa and $\pm 0.001 \le \Delta\varepsilon \le \pm 0.0025$.

While the determination of strains was done very carefully, sources of errors may still exist. One possible source of error is described. The pair of points, AB, chosen in Figure 7 should be along the tensile testing direction, but in reality, it may deviate slightly. Since the image has been magnified 250 times, the

deviation has to be quite significant to introduce a noticeable error in the strain measurements. In spite of this, we seek to verify our approach of strain measurements with a more conventional technique using strain gauges. A micro-specimen with aluminium strips was chosen. A strain gauge (EA-06-031CE-350, made by Measurements Group Inc.) was glued using an adhesive (M-Bond 200, made by Measurements Group Inc.) to the specimen within its gauge length and on the side not containing the aluminium strips. Tensile testing was then done. The stress-strain curve that resulted from the test is shown in Figure 8. Notice that the stress-strain curve based on the strain gauge gives a response, which is very close to that obtained by the current approach. However, we caution readers not to interpret the stress-strain curve in Figure 8 as the inherent mechanical response of the considered micro-specimen as the strain gauge could have introduced reinforcing effects in the specimen response. In addition, for comparison, we have included the stress-strain curve calculated based on crosshead displacements. The response turns out to be considerably softer (in terms of the flow stress levels) as it includes the "averaged" response of the specimen between the crossheads. The test results and discussions are given in the next section.

CHAPTER 5

TEST RESULTS AND DISCUSSIONS

The stress-strain curves for 10 micro-specimens have been shown in Figure 9. The data points for each curve are clearly shown; the curve itself is obtained by joining the data points using a smoothing routine in MS Excel.

While the stress-strain curves for most of the specimens are clustered together, the two lowermost curves are quite far from the remaining eight at the top. A possible reason in the spread in the top cluster of 8 curves may be due to the nature of the fiber distribution in the mat used to make the composite samples. Recall that the mat contains randomly oriented glass fibers; a visual examination of the sheet showed clearly that the fiber distribution is not uniform from one region to another. Therefore, it is quite possible that the fiber content may differ from one micro-specimen to another, leading to a possible variability in their stress-strain response too. Another possible reason could be non-uniformity in the orientation of the molecular chains in the polymers. However, we do not believe that such reasons are responsible for the significantly softer response of the two micro-specimens (the two lowermost curves in Figure 9). We have noted that the thickness of the stiffer 8 specimens (the top 8 curves) is in the range of 254 - 271.78 μm, whereas the thickness of the micro-specimens with a softer response

(the second curve from the bottom) was found to be 406.4 μm. This implies that the thick specimens had significantly more resin than the top eight, possibly leading to the softer response that appears in Figure 9. Paradoxically, the specimen corresponding to the lowest curve in Figure 9 has a thickness in the range of the ones corresponding to the top eight curves; we are yet to ascertain as to what reason(s) led to its significantly softer response.

The next phase of the research is to determine the effects of alcohol based fuels to FRPs. A representative behaviour of the FRP was obtained by testing the specimen after they were subjected to the following conditions:

1. Unexposed (or virgin) samples,
2. 3-day exposed samples,
3. 7-day exposed samples,
4. 3-day exposed and 3-day dried samples,
5. 7-day exposed and 7-day dried samples.

For each of the above conditions, multiple tests were carried out. Thus, for example, the multiple tests on virgin specimens (i.e. condition 1 listed above) resulted in stress-strain curves in Figure 10. A representative curve was then obtained from the multiple curves of Figure 10 by averaging the stress values corresponding to a given time. An identical procedure is followed for the strain.

The averaged stress and strain values is plotted and referred to as the "representative" response of the virgin FRP, and is given in Figure 11. As well, the standard deviation of the stress values from their average at a given time is computed with the length of the error bar taken as twice the standard deviation; an identical procedure is adopted for the strain values. The stress-strain curves from the multiple tests corresponding to the conditions 2-5 are given in Figs.12-15 respectively, and the procedure used for condition 1 is repeated to obtain the representative FRP responses for conditions 2-5. Note that the spread in the stress-strain curves in Figure 10 (as also in Figs.12-15) is significantly larger than those due to experimental errors in the current strain measurement technique (see last part of previous section). A strong possibility for such a spread is that the distribution of randomly oriented fibers in the as-received glass fiber sheets had a visible spatial non-uniformity. This may lead to a significant variation in the nature of fiber reinforcements among the micro-specimens tested, and thus a spread in the FRP response for each condition.

The representative stress-strain curves of the FRP under conditions 1-3 are given in Figure 16. The stress-strain curves of the exposed FRPs are significantly softer than that of the virgin FRP. As well, this strength reduction is non-monotonic with exposure time. Thus, exposure for 7 days actually results in a stronger FRP than the FRP exposed only for 3 days. The representative stress-

strain curves of the FRP under conditions 1, 4 and 5 are given in Figure 17, and a significant (but not total) strength recovery of the FRPs on drying after fuel exposure is obvious. To put the data of Figs.16 and 17 in an overall perspective, we have plotted the flow stress at a total strain of 1.5 % for each of the conditions 1-5; this is done in Figure 18. The lower and upper curves correspond to the flow stress of the exposed FRPs, and the exposed and dried FRPs respectively. Based on the obtained values, the strength loss on 3-day exposure is 92 %. Most of the loss is recovered on drying the sample for 3 days, resulting in a net loss of 19.7 %. As well, the exposed specimens become significantly more plasticized as indicated by the high strain values when compared to the virgin specimens. These results point to the possibility that there could be a significant loss in strength and increased plasticity of the FRPs as long as they are exposed to the alcohol-based fuels. The design process should account for this loss, regardless of the fact that the strength can be mostly recovered on drying the FRPs.

Another outcome of the experiments, which is of some importance, is that the flow stress for the 7-day exposed samples is somewhat higher than that of the 3-day exposed samples (see lower curve of Figure 18). A similar effect on the flexural modulus was found by Kamody et al.[8], and the possible reasons they cited were continuous curing and experimental errors. While, in principle, the same reasons may hold here, we do not really expect continuous curing in our

experiments because the ambient temperature (20°C) in which the entire set of experiments has been done is quite moderate. Further, the difference in the flow stresses of the 3-day and 7-day exposed samples that we see in Figure 18 is most certainly higher than the experimental errors in the stress measurement. In our view, a possible reason is that the identical crosshead displacement rate of 0.508 mm/min used for all the tests may in fact cause a stiffer response. This is due to higher rate dependence that results in higher flow stress in more saturated specimens (the 7-day specimens) as compared to that in less saturated specimens (the 3-day specimens). While the same qualitative feature may be observed for exposed and dried samples (see upper curve of Figure 18), the effect is expectedly not as pronounced. We hope to confirm this hypothesis in the future.

CHAPTER 6

CONCLUSIONS AND FUTURE WORK

In this dissertation, we have reported an experimental approach to determine extensional strains in composite tensile micro-specimens (nominal thickness 254 μm). This has been accomplished by sputter deposition of aluminium strips along the gauge width of a micro-specimen, and then using a non-contact optical method to track the changes in aluminium strip dimensions during the loading process. A partial validation of the developed approach was obtained by comparing its predictions with more conventional strain-gauge measurement techniques. Further, we have carried out qualitative surface analysis of micro-specimens exposed to a 50-50 volumetric mixture of methanol-ASTM Fuel C using Scanning Force Microscopy, and have found that there is almost no deterioration of the condition of aluminium strips. Thus, the developed method for strain measurements may also be used for micro-specimens exposed to methanol-based fuels.

This dissertation further reports preliminary experimental results on the effects of exposure of fiber-reinforced plastic (FRP) tensile micro-specimens to a 50-50 volumetric mixture of methanol and ASTM Fuel C under ambient conditions (20 ^{o}C). We have found that the flow stress of the specimens exposed

to the fuel for 3 day and 7 day periods become significantly weaker in their tensile response compared to the response of virgin (or unexposed specimens). However, on drying the exposed specimens for an identical period of time leads to a significant recovery. These results point to the possibility that FRP-based structures exposed to alcohol-based fuels (e.g. underground fuel storage tanks) may need to account for property changes of the FRP during service. This is regardless of the fact that the changes can be significantly recovered when the FRP is dried for an appropriate period of time. In the future, this preliminary work needs to be extended to a wider study where the influence of other parameters - specimen thickness, type of alcohol, alcohol/fuel ratio, pressure and temperature - on the FRP tensile response is studied. Furthermore, the effect of the aforementioned properties on the flexural response should also be examined.

REFERENCES

1. R.R. Skabo, L.H. West, 1966, Evaluation of Corrosion Resistance, Detroit, Michigan.
2. K.C. Garrity, 1986, Cathodic Protection of Underground Storage Tanks, Sigma Magazine.
3. J.H. Pim, 1988, Tank Corrosion Study, Suffolk County, Department of Health Services, Office of Underground Storage Tanks, U.S. EPA.
4. Causes of Release from UST Systems, U.S. EPA/Office of Underground Storage Tanks, Sept. 1987, pg. 11-14.
5. B. Bodger, 1990, Review of Internal Corrosion of Underground Fuel Storage Tanks, Amoco Chemical Co., Research and Development Department, Naperville, IL.
6. Underground Storage Tanks, Technical Requirements and State Program Approval: Final Rules, 40CFR Parts 280 and 281, U.S. EPA, September 1988.
7. J.H. Fitzgerald, 1988, Materials Performance, Vol. 27, No. 4, pg. 36-40.
8. J.F. Kamody, A. Damiani, and R.J. Stadelman, 1994, The use of FRP with Alcohol-Containing Fuels, Journal of Reinforced Plastics and Composites, Vol. 13, pg. 213-236.
9. P. Stapleton, 1987, Sweden Report, UST2-5-SB-22B, U.S. EPA.

10. ASTM D638M-93: Test Method for Tensile Properties of Plastics (Metric), Annual Book of ASTM Standards, 1996, 08.01, American Society of Testing Materials, PA.

11. J. Crank, The Mathematics of Diffusion, Second Edition, Oxford Science Publishings, 1975, pg. 21

12. J.W. Chin, T. Nguyen, and K. Aouadi, 1997, Effects of Environmental Exposure on Fiber –Reinforced Plastic (FRP) Materials Used in Construction, Journal of Composites Technology and Research, Vol. 19, No. 4, pg. 205-213.

13. L. Prian, and A. Barkatt, Chemical, Thermochemical, and Mechanical Studies of FRP Degradation in Corrosive Environments, Corrosion 1998, March 1998, San Diego, CA, Paper No. 455.

14. L. Prian, and A. Barkatt, 1999, Degradation mechanism of fiber-reinforced plastics and its implications to prediction of long term behavior, Journal of Materials Science, Vol. 34, pg. 3977-3989.

15. L.J. Craigie, M.J. Svatek, M.N. White, Development of Composite for Underground Gasohol Storage Tanks, Corrosion 1986, March 1986, Houston, TX, Paper No. 282.

16. C.C. Perry, 1985, Strain-Gage Reinforcement Effects on Low-Modulus Materials, Experimental Mechanics, Vol. 9, No. 5, pg. 25-27.

17. D.J. Goertzen, 1992, A Soft Tissue Test Apparatus with Application to the Knee Joint Meniscus, M.Sc. Thesis Dissertation, University of Alberta, Canada.

APPENDIX

PREPARATION OF MASK FOR SPUTTERING

The mask used for sputter deposition of aluminium strips (see Sec.2.2) on the composite sheets is prepared from 0.001 in. thick brass shimstock manufactured by Precision Brand Ltd. The brass shimstock is sprayed with photoresist (supplied by DATAK Ltd.) on both sides, and then dried for 24 hours in a dryer. This is followed by exposing an assembly of glass sheet, film transparency, brass shimstock, and cardboard sheet on the glass side to ultraviolet light for 5 minutes. Here, the film transparency has two black strips with nominal dimensions corresponding to the aluminium strips that are to be sputtered onto the composite sheets (see Figure 3(a)). The brass shimstock is then exposed to a developer (supplied by DATAK Ltd.) for 1 minute; this removes the photoresist from the areas on the shimstock corresponding to the black strips on the transparency. The shimstock is then dried in the dryer for 3-4 hours, and then etched for 7 minutes in ferric chloride. The areas of the shimstock corresponding to the black strips (on the film transparency) are etched away, resulting in the brass mask shown in Figure 3(b).

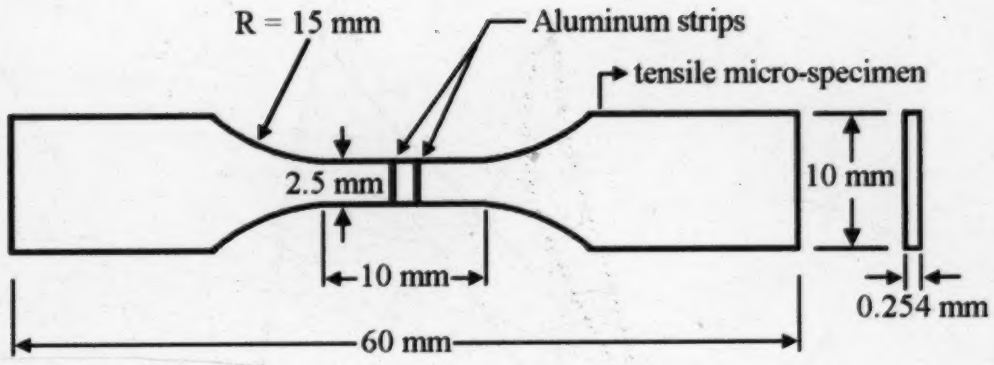

(a)

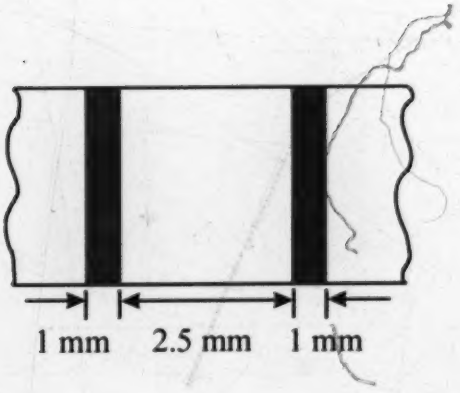

(b)

Figure 1(a). Schematic of the tensile micro-specimen, with dimensions conforming to ASTM D638M-93, (b) enlarged view of the gauge section.

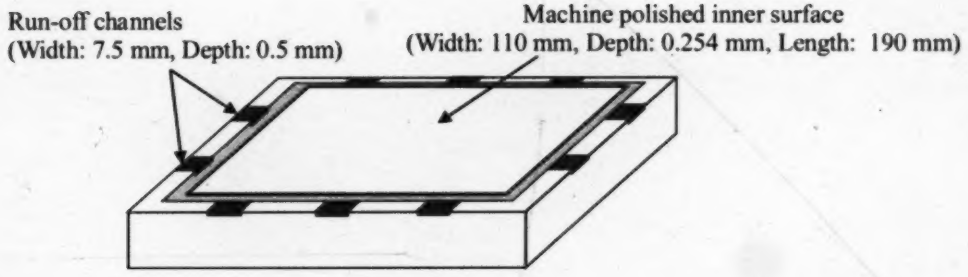

TOP

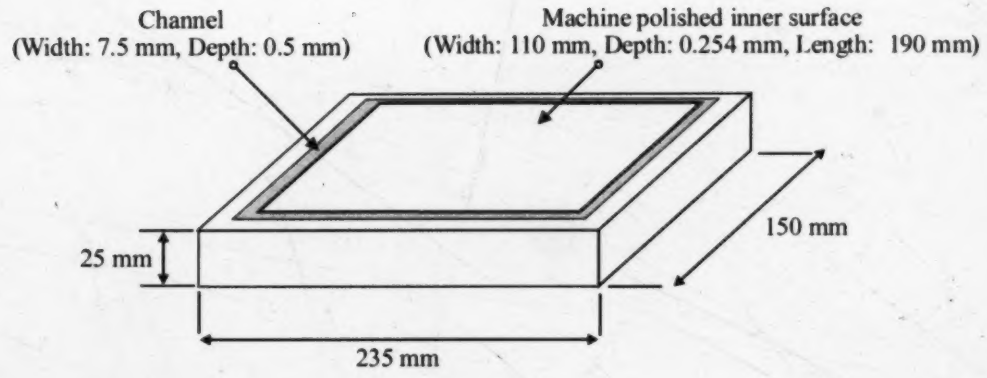

BOTTOM

Figure 2: Schematic of the top and bottom parts of the steel mold used to make fiber-reinforced composite sheets. The mold is assembled by mating the upper surface of the top part to the upper surface of the bottom part.

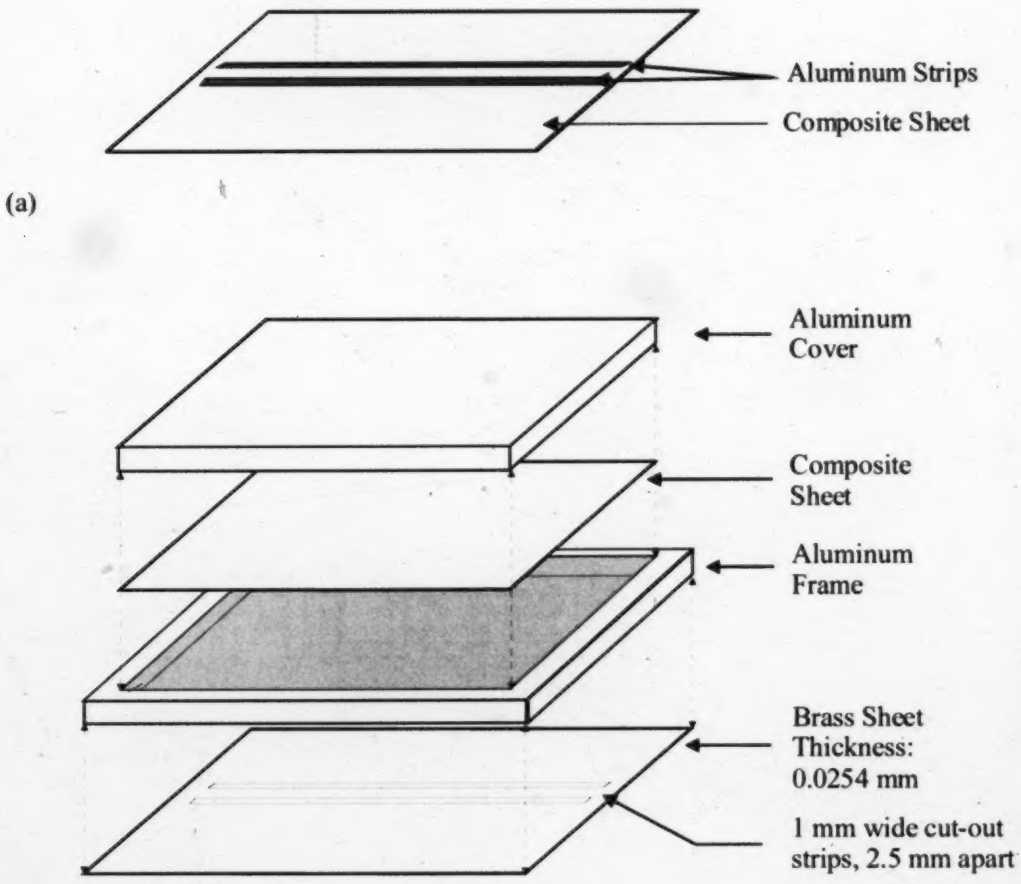

Figure 3. (a) Schematic of a composite sheet with two aluminum strips,
(b) An exploded view of the assembly used to produce the sputtered sheets.

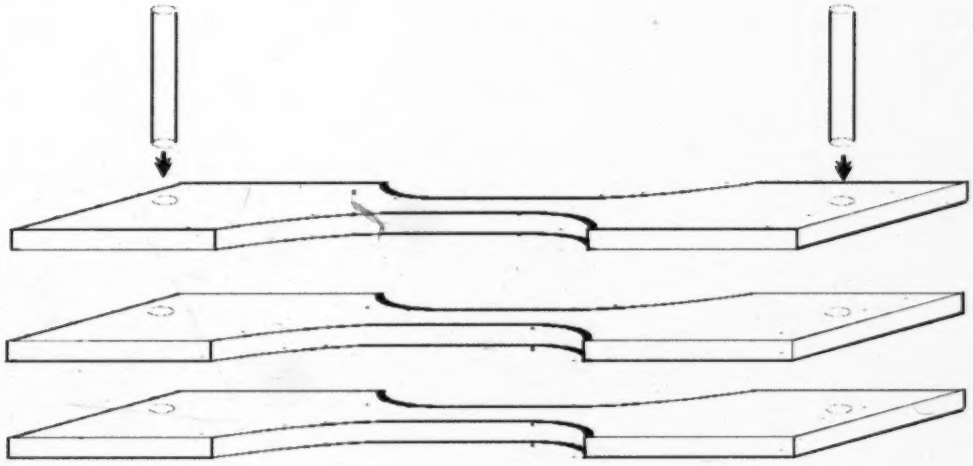

Figure 4. Schematic of the template used to cut the tensile micro-specimens.

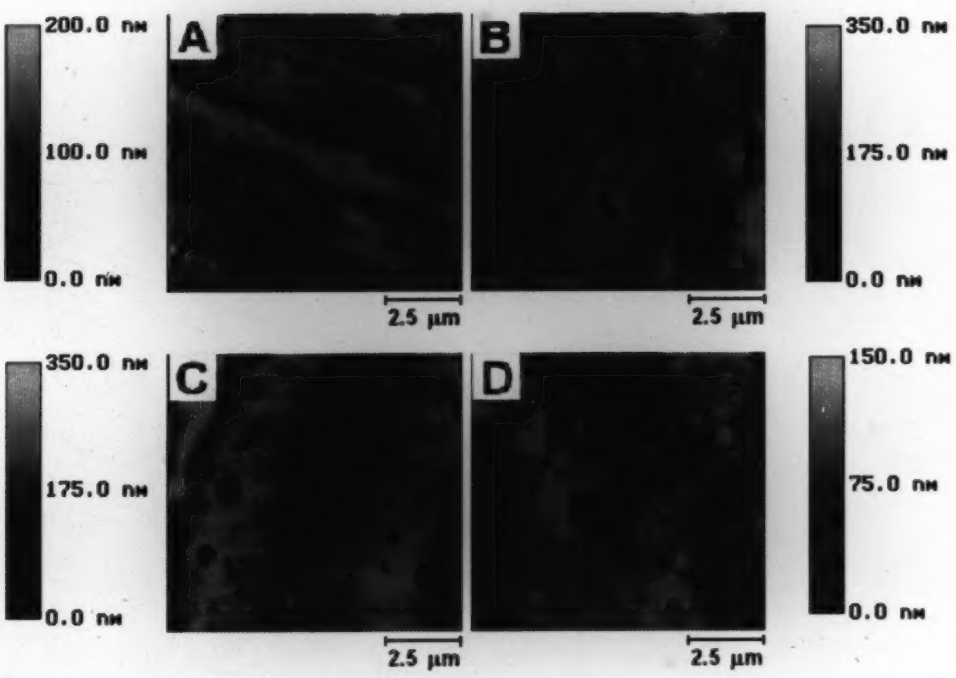

Figure5. Scanning Force Microscopy (SFM) images:

A. Bare surface of a composite sheet before exposure to alcohol-based fuels,
B. Aluminium covered surface of a composite sheet before exposure to alcohol-based fuels,
C. Bare surface of a composite sheet after 7 day exposure to a volumetric mixture of 50%-50% methanol-ASTM Fuel C,
D. Aluminium covered surface of a composite sheet after 7 day exposure to a volumetric mixture of 50%-50% methanol-ASTM Fuel C.

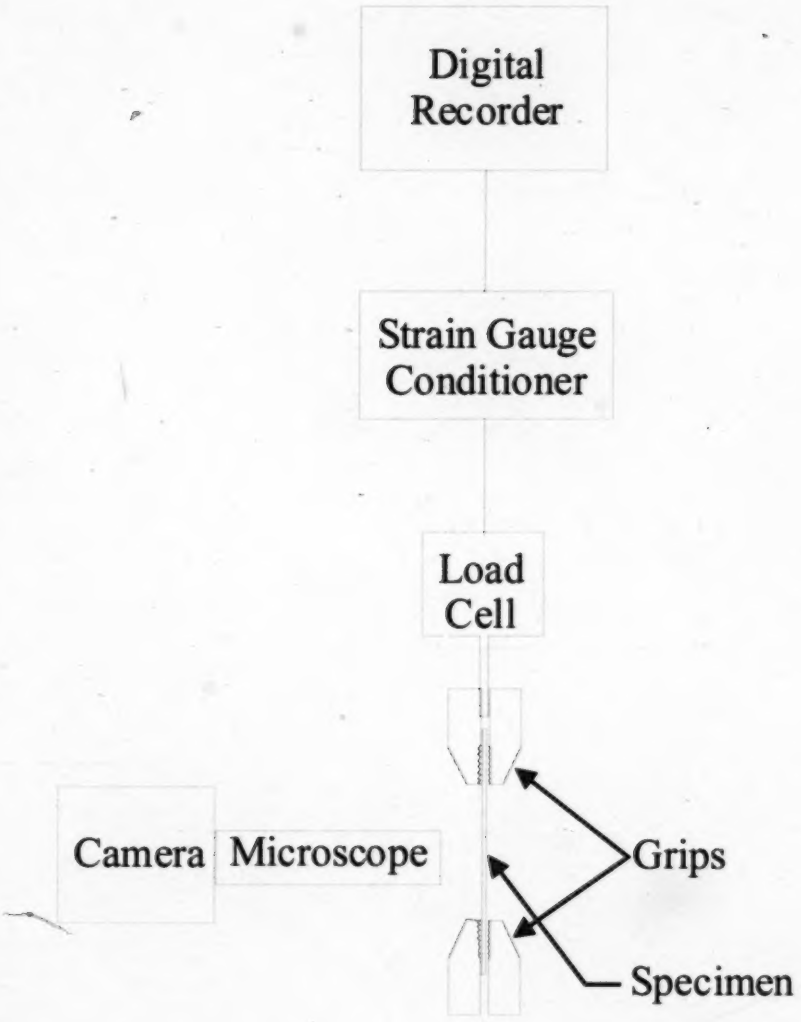

Fig 6. Schematic of the configuration to test tensile micro-specimens.

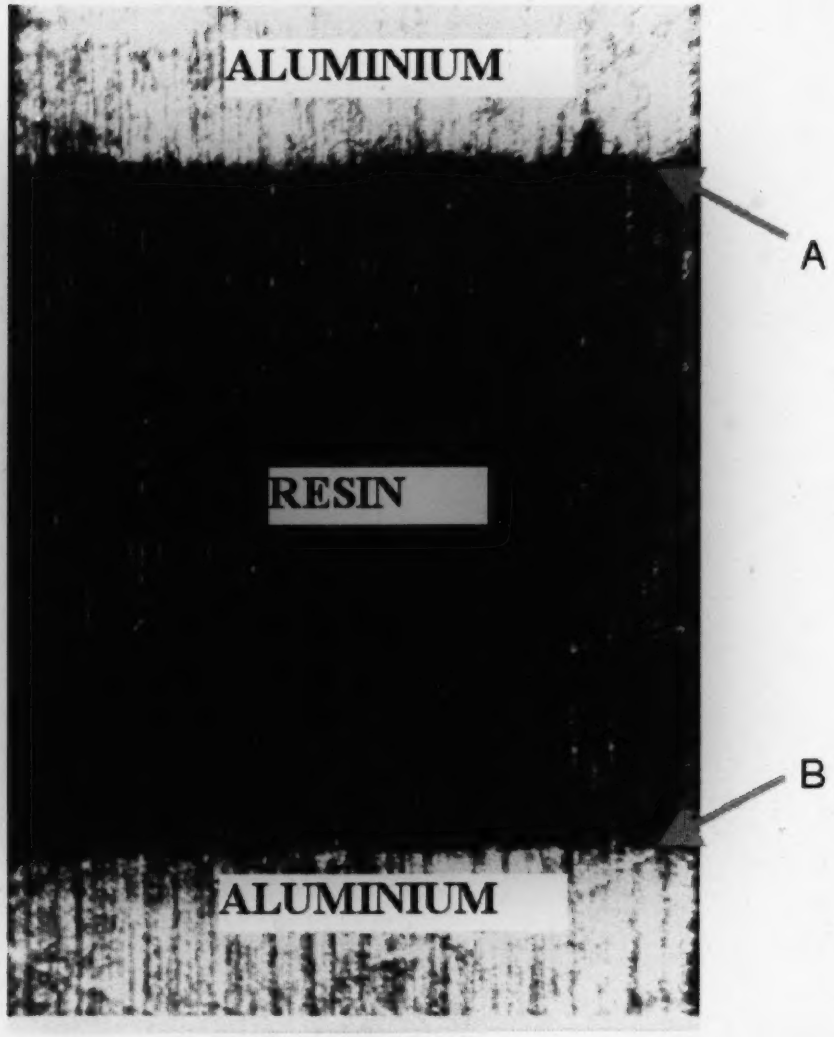

Figure 7. A scanned image of the aluminum strip-covered surface of a tensile micro-specimen.

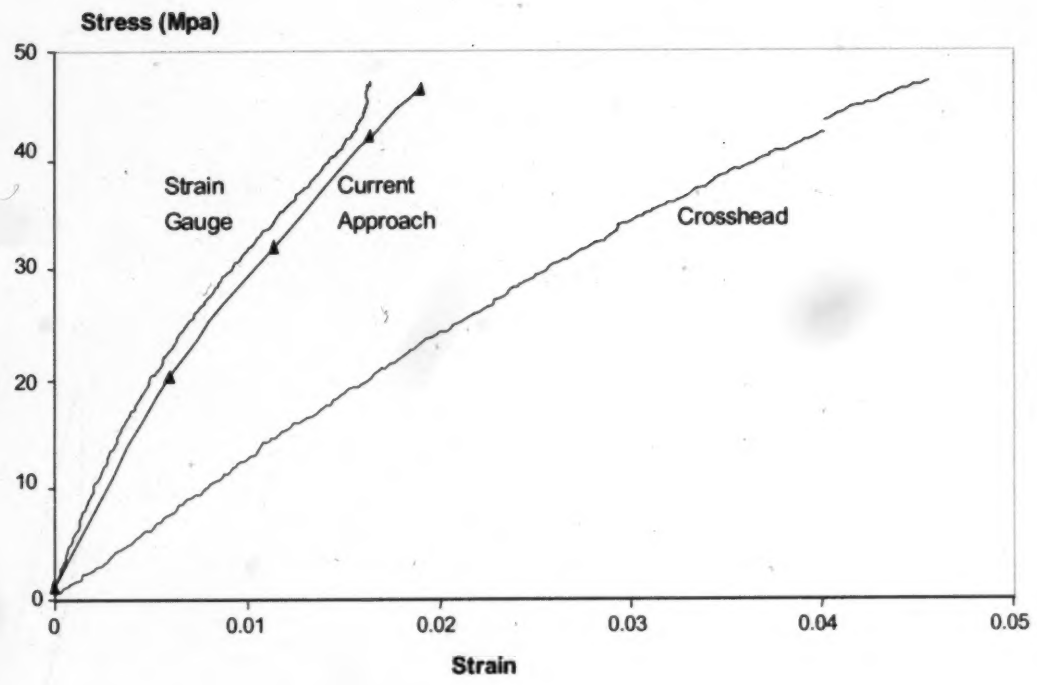

Figure 8. Stress-strain curves obtained for the same micro-specimen based on strain gauge measurements, the current approach and crosshead displacements.

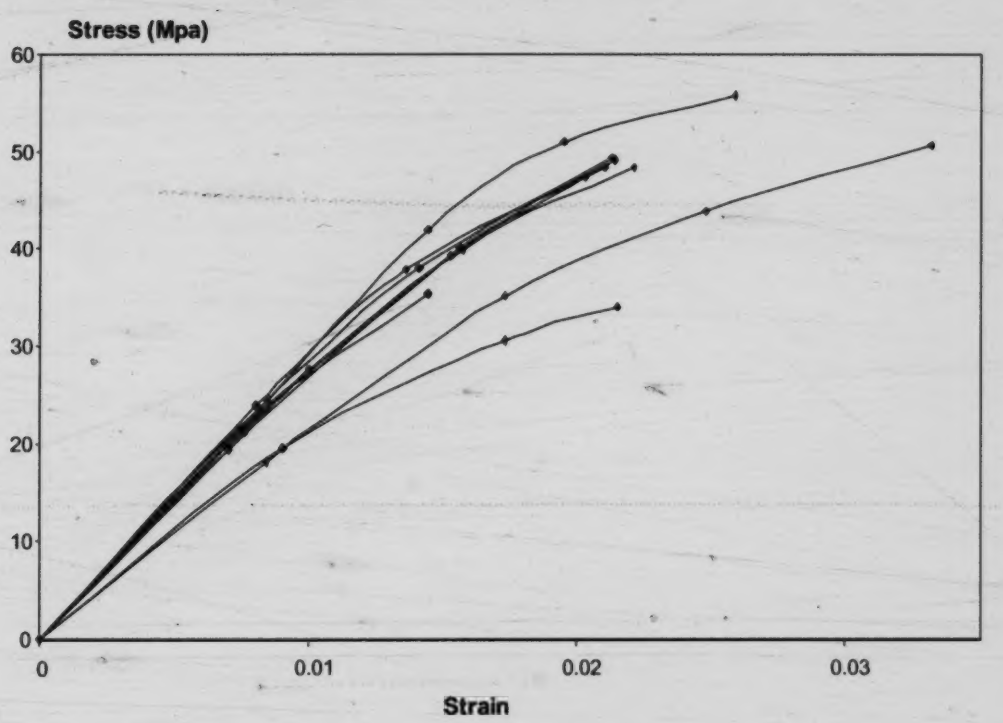

Figure 9. Stress-strain curves obtained by the current approach for 10 different micro-specimens.

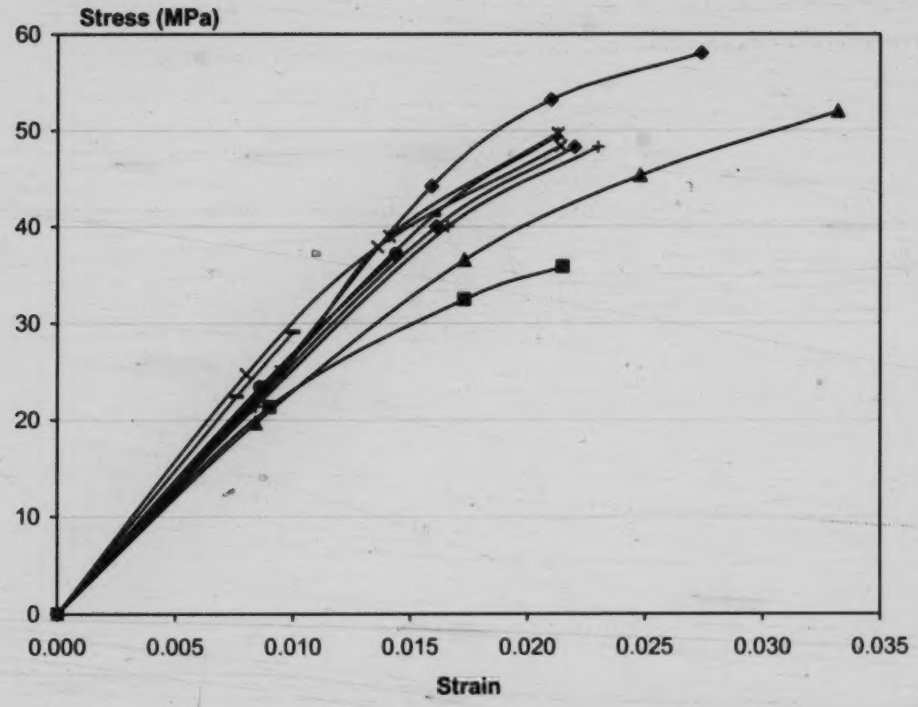

Figure 10: Individual stress-strain curves of virgin micro-specimens. Each micro-specimen was tested to failure.

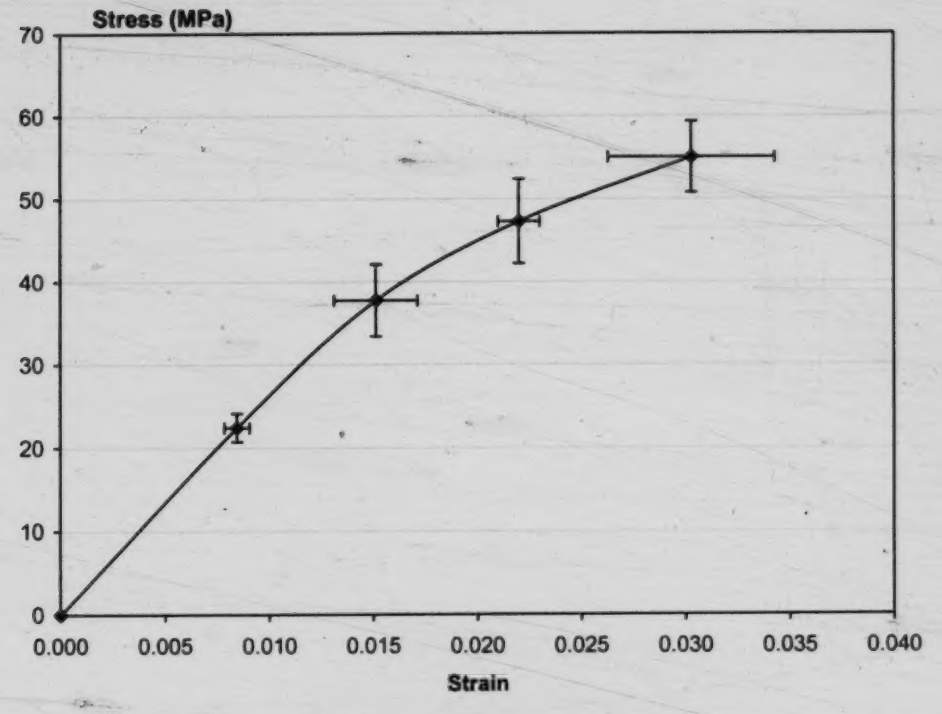

Figure 11: The representative stress-strain curve of the virgin FRP.

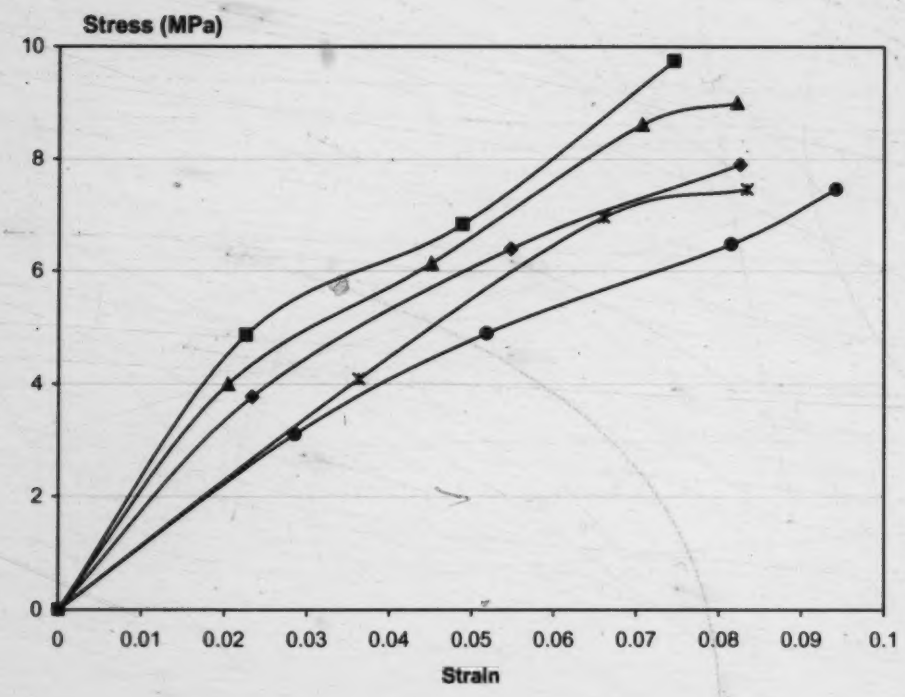

Figure 12: Individual stress-strain curves of micro-specimens after 3-day exposure to fuel mixture. Each micro-specimen was tested to failure.

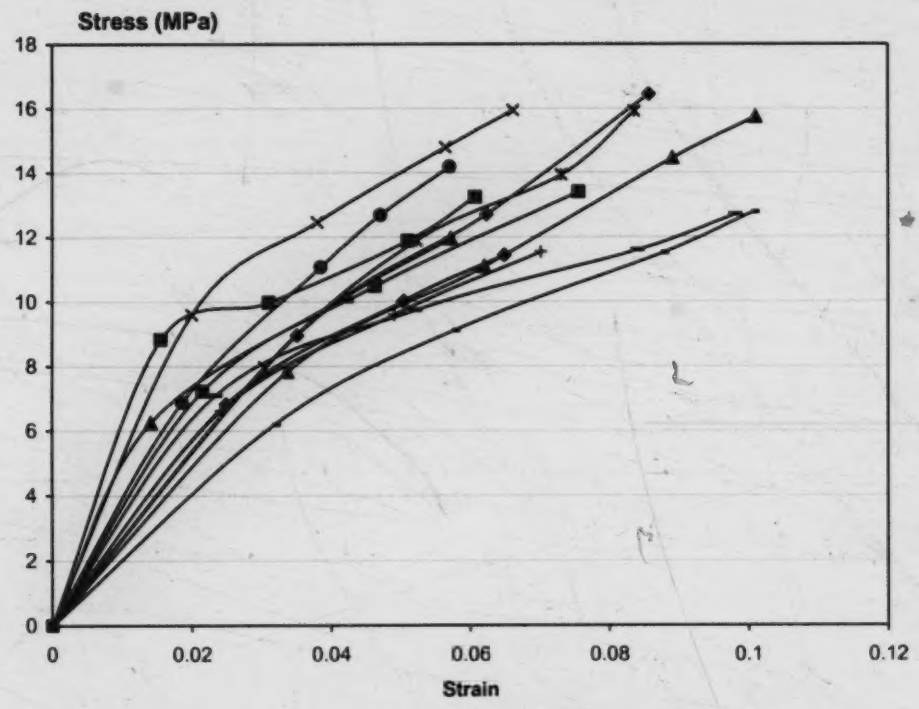

Figure 13: Individual stress-strain curves of micro-specimens after 7-day exposure to fuel mixture. Each micro-specimen was tested to failure.

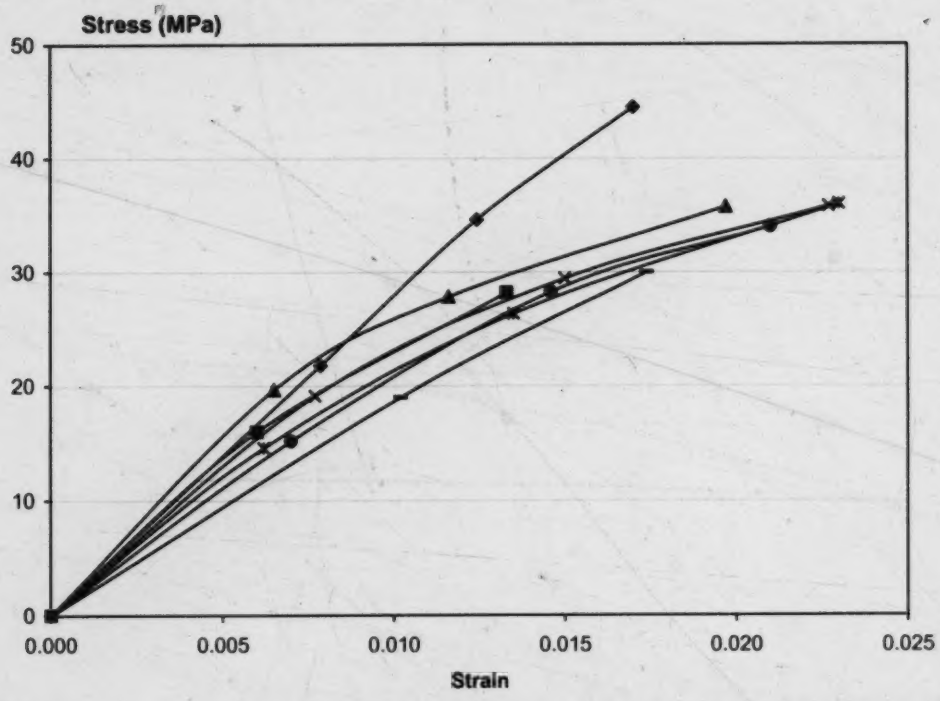

Figure 14: Individual stress-strain curves of micro-specimens after 3- day exposure to fuel mixture and then drying for 3 days. Each micro-specimen was tested to failure.

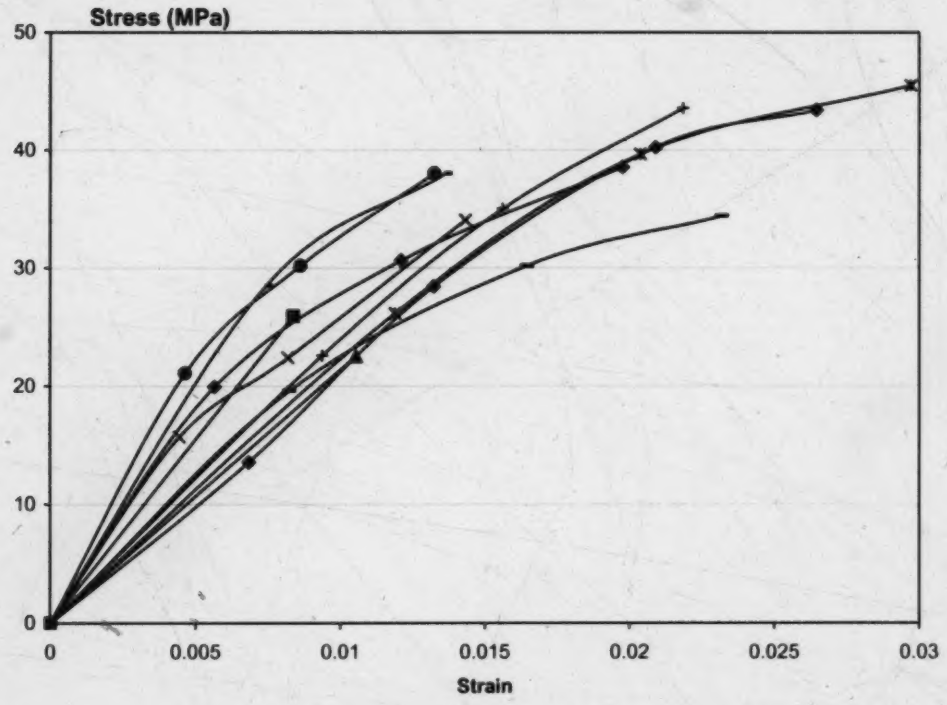

Figure 15: Individual stress-strain curves of micro-specimens after 7-day exposure to fuel mixture and then drying for 7 days. Each micro-specimen was tested to failure.

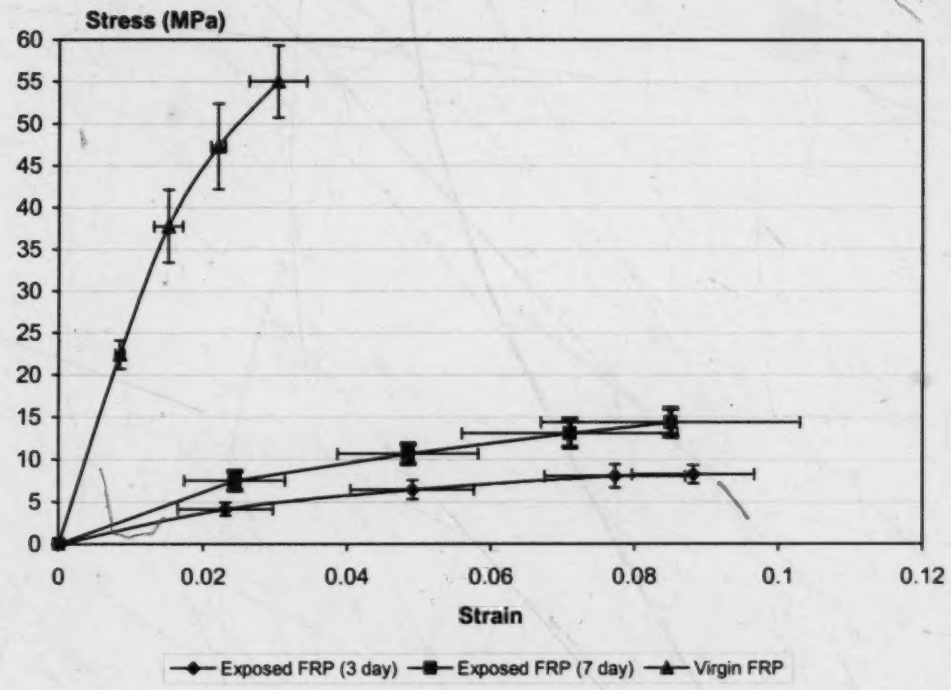

Figure 16: The representative stress-strain curves of the exposed FRPs.

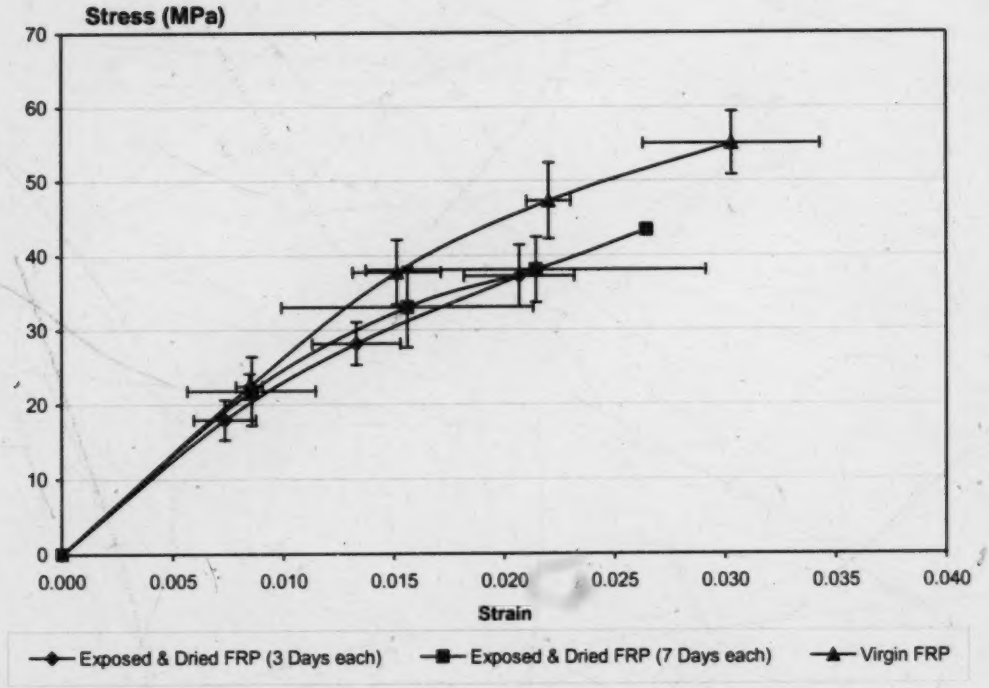

Figure 17: The representative stress-strain curves of the exposed & dried FRPs.
*Note: The last point has only one recorded data point for Exposed & Dried FRP (7 Days each).

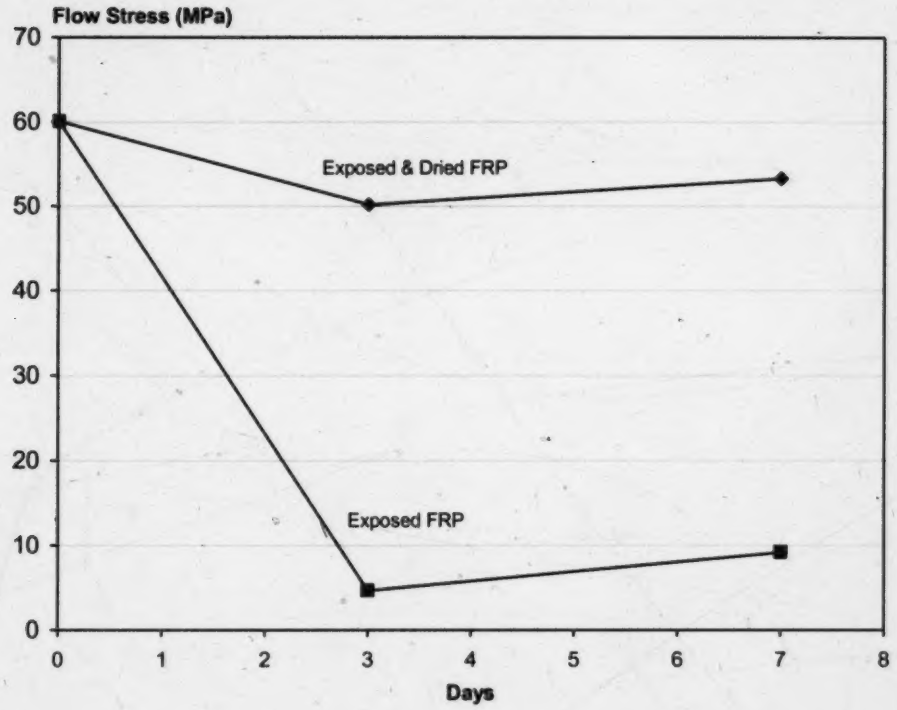

Figure 18: Dependence of the FRP flow stress (at 1.5% strain) on fuel exposure time.